Acidus electricus: pH dependence of growth and the electrical properties of the algal Chlorophyte *Eremosphaera viridis*[1].

Sandra Khine[2] and Roger R. Lew, Biology Department, York University

Revision 2.20 (04 October 2010)

OBJECTIVE

To determine the pH dependence of growth and electrical properties in the green unicellular alga *Eremosphaera viridis*.

[2] RAY (Research at York) Research Assistants. Experiments were performed 01MAY2010 through 31AUG2010 in the Lew Laboratory (RRL email: planters@yorku.ca) and were funded in part by NSERC (Natural Sciences and Engineering Research Council)

INTRODUCTION

The alga *Eremosphaera viridis* is a well known model organism for studies of ion transport, and inter-organellar regulation of pH. This is due in part to the large size of the individual cell (about 120 micron) and its simple spherical geometry which makes it amenable to a variety of micro-manipulation techniques. These techniques include electrophysiological measurements of the plasma membrane (Köhler et al., 1983, 1985, 1986) and the vacuolar membrane (Bethmann et al., 1995; Linz and Köhler, 1994). In depth characterization of pH regulation is also possible, using intracellular pH probes (Bethmann et al., 1995, 1998; Bethmann and Schönknecht, 2009). Even pressure measurements can be made (Freyer, 1988), and the cells can be micro-injected.

In Canada, *E. viridis* inhabits acid (low pH) lakes, so it is part of the acid-challenged aquatic ecosystems that are of considerable environmental interest (Dillon et al, 1987). In this report, we confirm the acidophilic nature of the alga with respect to growth, and measure the effect of eternal pH on the plasma membrane potential (after first exploring the effect of impalement and current injection into the cell).

The *E. viridis* cell membrane potential is dependent on potassium, sodium, calcium, and hydrogen ions (Köhler, 1985). It is possible to calculate cell membrane potentials at different pH knowing the concentration of the other ions inside and outside of the cell. Using the Goldman-Hodgkin-Katz (GHK) voltage equation, we can approximate the membrane potential over a range of proton concentrations ($[H^+]$)[3], when net membrane current of all ion species is assumed to be zero (Schultz, 1980):

$$E_m = \frac{k_B T}{e} \ln\left(\frac{P_{Na}\left[Na^+\right]_o + P_K\left[K^+\right]_o + P_{Cl}\left[Cl^-\right]_i + P_H\left[H^+\right]_o}{P_{Na}\left[Na^+\right]_i + P_K\left[K^+\right]_i + P_{Cl}\left[Cl^-\right]_o + P_H\left[H^+\right]_i}\right)$$

Where E_m is membrane potential in Volts, k_B is the Boltzmann constant, T is temperature in Kelvin, and *e* is the electron charge. P_{Na}, P_K, P_{Cl}, and P_H are the permeability coefficients. These are not necessarily known, but the GHK equation can be modified to use permeation ratios, the ratios can be obtained from the literature: $P_{Na}/P_K=0.3$, $P_{Cl}/P_K=0.1$, $P_H/P_K=100$ (Köhler, 1985).

The following are average internal concentration of ions: sodium 0.050M, potassium, potassium 0.120M, chloride 0.0065M, and proton 10^{-7}M (based on assumed cytoplasmic pH of 7.0) (Köhler, 1985). External concentrations of ions are based on APW solution make-up (Table III): sodium 0.0005M (but slightly variable because NaOH is used to modify the pH of the APW solutions), potassium 0.0005M, chloride 0.0014M, and hydronium concentration changes depending on pH of APW. Substituting these concentrations and ratios of relative permeation coefficients into GHK we obtain a relation of membrane potential to H^+ concentration (Figure 1).

[3] The 'real' form of H^+ in aqueous solution is the hydronium ion (H_3O^+) but we will follow the convention of describing it as a proton (H^+).

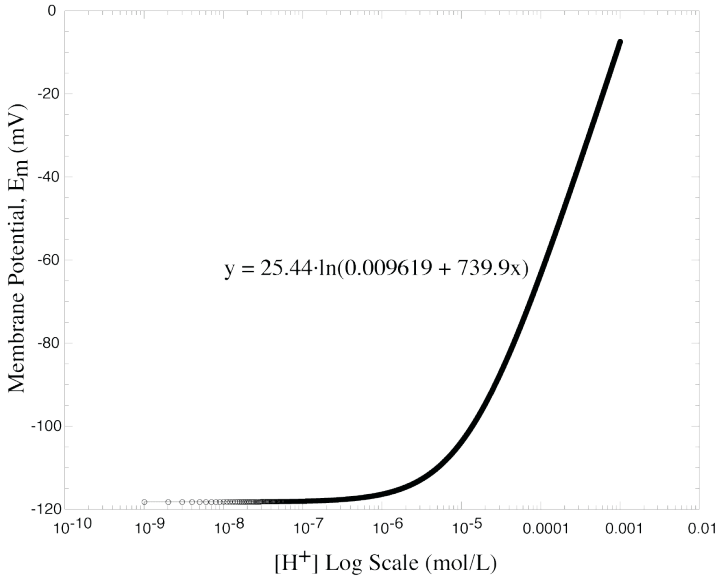

Figure 1. GHK derived plot of membrane potential over varied proton concentration. The following is a graph of the resultant function for membrane potential, E_m, over range of proton concentration, $[H^+]$ deduced from reducing the GHK relationship with known values of internal and external concentration, ratios of permeable coefficients, and temperature.

The objective of our research was to explore the effect of $[H^+]$ on both algal growth and the cell's electrical properties (voltage and resistance).

MATERIALS AND METHODS

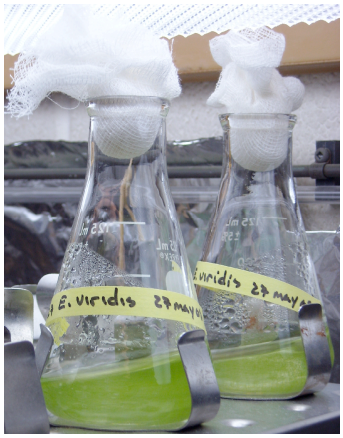

Algal Strain. The algal *Eremosphaera viridis* de Bary strain used in this project was collected at Plastic Lake (Ontario) in 1987 and is maintained at the Canadian Phycological Culture Centre (CPCC 127, formerly UTCC 127). The strain is designated LB (live bacteria). The stock used for the pH perfusion and growth experiments was grown under T8 fluorescence lamps (photon flux 50 μmol m^{-2} s^{-1}) on a rotary shaker (120 rpm) in 125 or 250 ml Ehrlenmeyer flasks containing 25 or 50 ml of Bold's basal medium (BBM) supplemented with vitamins (Table I). Samples or transfers were taken from cultures that were one to two weeks old.

Table I: Bold's basal medium composition.

Salt (stock)	MW	Dilution	Final concentration
KH_2PO_4 (1.75 g/100 ml)	136.09	0.01	1.29 mM
$CaCl_2 \cdot 2H_2O$ (0.25 g/100 ml)	147	0.01	0.17
$MgSO_4 \cdot 7H_2O$ (0.75 g/100 ml)	246.5	0.01	0.30
$NaNO_3$ (2.5 g/100 ml)	84.99	0.01	2.94
K_2HPO_4 (0.75 g/100 ml)	174.2	0.01	0.43
NaCl (0.25 g/100 ml)	58.44	0.01	2.99
$Na_2EDTA \cdot 2H_2O$ (1.0 g/100 ml) KOH (0.62 g/100 ml)	372.24 56.11	0.001	0.027 0.11
$FeSO_4 \cdot 7H_2O$ (0.498 g/100 ml) H_2SO_4 (conc. 18 M) (0.1 ml/100 ml)	278.0 98.08	0.001	0.018 0.00018
Trace Metal Solution	*see below*	0.001	*see below*
H_3BO_3 (1.15 g/100 ml)	68.13	0.0007	0.012
Vitamins		0.000025	
Trace Metals (g/100 ml, *MW*, final concentration [**μM**]): H_3BO_4 (0.286, *68.13*, **42.0**), $MnCl_2 \cdot 4H_2O$ (0.181, *197.92*, **9.1**), $ZnSO_4 \cdot 7H_2O$ (0.0222, *287.54*, **0.77**), $Na_2MoO_4 \cdot 2H_2O$ (0.039, *241.95*, **1.6**), $CuSO_4 \cdot 5H_2O$ (0.0079, *249.7*, **0.31**), $Co(NO_3)_2 \cdot 6H_2O$ (0.00494, *291.03*, **0.17**)			
Vitamins (g/10 ml): Thiamine•HCl (0.1), Vitamin B_{12} (0.002), Biotin (0.001)			

pH Dependence of Growth Experiments. Two growth experiments were conducted using the same protocol and light conditions but with different stock algal cultures and different pH ranges. In the first experiment (25 June 2010 through 24 July 2010), the algae were grown at pHs 5, 6, 7, 8, and 9 using three replicate flasks (125 ml). In the second experiment, the algae were grown at pHs 3, 4, 5 and 6. (29 July 2010 through 23 August 2010), again with three replicate flasks. The culture solutions were modified Bold's basal medium (Table I) as described below.

For both experiments, the cells were grown under T8 fluorescence lamps on a rotary shaker (120 rpm) in 125 ml Ehrlenmeyer flasks containing 25 ml of Bold's basal medium (BBM) supplemented with vitamins (Table I) plus 50 mM of buffer (Table II). Buffers were selected on the basis of having a pK_a that was near the final pH of the culture medium. The pH of the BBM-buffer solutions was adjusted with NaOH, then filtered sterilized and 25 mL added to each of the three flasks for each pH. The flasks were inoculated by adding 2 mL of cells from a stock *Eremosphaera viridis* cell culture. The cells are large and heavy, so they tend to settle to the bottom of the flasks quickly. So, the

stock flask was stirred vigorously prior to removing the 2 mL aliquot to ensure the same number of cells was transferred to each of the treatment flasks. Sterile technique was used in transferring all solutions and algae. This involved working in a sterile laminar flow hood, flaming the lips of the flasks and the pipettes used for transfers, as required.

Table II: Buffer for Growth Experiment

pH	Buffer	pKa	Molecular Weight (g/mol)	50 mM (g/L)	50 mM (g/250mL)
3	Phthalic acid	2.95	166.13	8.31	2.08
4	Phthalic acid	5.41	166.13	8.31	2.08
5	MES	6.15	195.23	9.76	2.44
6	MES	6.15	195.23	9.76	2.44
7	MOPS	7.2	209.26	10.46	2.62
8	TES	7.5	229.25	11.46	2.87
9	TAPS	8.4	243.20	12.16	3.04

Cell Counting Protocol. Because of the large size and weight of the cells, and their relatively low density, a hemacytometer could not be used very effectively. Instead, to determine the cell population in a flask, samples of 2µL to 50µL were taken using either a Pipetteman P200 pipette or a Drummond 10µL displacement pipette. The volume was selected to obtain a relatively consistent number of cells for counting. To obtain a representative sample, the flask was stirred vigorously to ensure the cells were in suspension and well-mixed before a sample was taken. The samples were placed on the lids of culture dishes (35 X 10 mm), and the cells in each droplet counted using a X10 objective. The number of cells per droplet was divided by the volume of the droplet to calculate the cell density (cells/mL). At least three samples were taken from each flask for counting to improve accuracy. The cell density of the stock flask used to inoculate the treatment flasks was determined the same way. Cell count measurements were taken approximately once a day.

Electrophysiology. To determine the electrical properties of the cell, double barrel micropipettes were used. This made it possible to inject current through one barrel, and monitor the voltage deflection through the other barrel. Thus, in addition to measurements of the electrical potential, the resistance of the cell could be determined, and from the size (area) of the cell, the specific resistance ($\Omega\ cm^2$). A WPI duo773 electrometer was used for current injection and voltage monitoring. The magnitude of the current was ± 1 or ± 2 nA. The current and voltage outputs of the electrometer were digitized with a USB-6009 (National Instruments) data acquisition module using nidatalogger in LabView (National Instruments). The electrometer was also connected to a Tektronix TDS210 Oscilloscope to monitor signals during impalements and resistance measurements. Details of the micropipette fabrication, cell impalements and perfusion are described below.

Double-Barrel Micropipette Fabrication. The micropipettes were fabricated as described in Lew (2006). Briefly, two glass blanks were placed in the pipette puller, heated, twisted 360°, and pulled to a point. Fast-setting epoxy glue was applied above the twist for reinforcement. When the epoxy had set, one barrel was bent outwards at

approximately 30° by heating point over micro-burner (Figure 2).

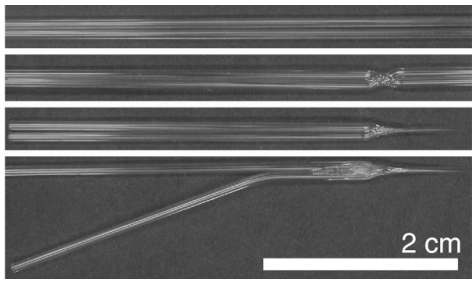

Figure 2. Preparing double-barrel micropipettes. After preparation, the micropipette is filled with 3M KCl solution and placed into microelectrode holder.

Micropipette Preparation. The tip of the double-barrel micropipette was filled by placing a small amount of the 3M KCl solution in the barrels using a 33 Gauge needle syringe. After a few moments (after the tip was filled with solution by capillary action) the barrels were completely filled with 3 M KCl using the fine gauge needle. The straight barrel of the double-barrel micropipette was inserted into the microelectrode holder (WPI Holder Half Cells 1.0 mm) that was pre-filled with KCl. Care was taken to ensure there were no large bubbles in the barrel or holder. A chlorided silver wire (0.25 mm diameter) was inserted into the bent barrel. The holder with double-barrel micropipette was attached to one of the headstages of the electrometer, and the silver wire attached to the other headstage with an alligator clip.

Impalement Preparation Protocol. Before impalement, 0.5 mL of *Eremosphaera viridis* cells were placed in a test tube and washed three times with at least 5 mL of APW7 by letting the cells settle to the bottom and removing the excess solution twice. The cells are allowed to settle and 3 mL of the cells at the bottom of the tube were transferred to the lid of Petri dish (35 X 10mm). Two opposite points on the lid were marked to help align the placement of perfusion intake and outtake tubes and the height of the solution was marked as an indicator of stable perfusion during the experiment.

Micro-Injection Set-Up. The cells are viewed and impaled under X10 objective on a Zeiss Axioskop microscope. The condensor light was filtered through a flat flask containing 3.5% $CuSO_4 \bullet 5H_2O$ (this blocks infrared light and transmits PAR — photosynthetically active light— in the range 400 to 700 nm). The light intensity was measured with a radiometer probe and set as close to 50 μmol m^{-2} sec^{-1} photon flux) which is the same as the light intensity used for culturing the cells.

Determining Perfusion Rate. Since the effect of pH changes was going to be examined, we needed to determine how long it took for perfusion solution to be completely replaced by letting the desired solution flow into the dish from an intake tube on one side of the objective, and removal of the previous solution by an outtake tube on the other side of the objective. The rate was determined by filling the dish with water and perfusing in a dye solution (10 μL of 200 mg/mL of Na•fluorescein diluted in 50mL of water). Perfusion was performed using a Bio Rad Econo peristaltic pump. Pre-cut silicone tubing of 1.6 mm for inflow and 3.2mm for outflow were used to ensure the outflow rate did not lag behind the inflow rate. Silicone tubing of diameter 0.3175cm was used to connect the pump to the inflow and outflow ports at the dish (using bent glass tubes) and to the

perfusion solutions. The glass tubes were placed directly on either side of dish with the inflow slightly under the water and outflow slightly closer to surface.

During perfusion runs, samples of 0.5mL are taken from the middle of the dish (where the cells would be held and impaled) at 5s, 10s, 15s, 20s, 40s, 1min, 1min 20s, 1min 40s, and 2min. The samples are diluted with 1.0mL of water into a 1.5mL cuvette. The dye concentration was measured as absorbance at 495 nm (the maximal aborbance wavelength of fluorescein) (A_{495}) using a spectrophotometer. The A_{495} is the ratio of the voltage output of the V_{blank} (dH_2O) to the V_{sample} ($A_{495} = -\log(V_{sample}/V_{blank})$. The A_{495} of the perfusion samples are plotted *versus* time in Figure 3.

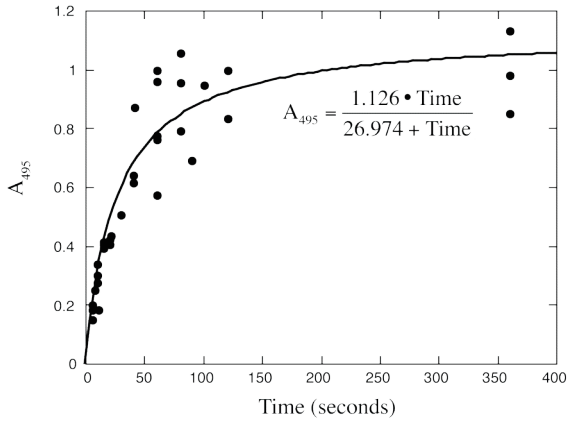

Figure 3. Evaluation of mixing during dish perfusion. Data are fit to a hyperbolic function. The A_{495} for the final concentration (measured separately) was set at 360s. Large variability was due to using a P200 pipetteman to pipette 10μL of Na•Fluorescein for dilution instead of the more accurate P20.

From the trials (Figure 3), after 120s almost 90% of the final concentration of dye solution was achieved. Therefore, 2min was selected as the time it would take to change from one pH solution to another. One trial of reversing dye to water also yielded consistent result of A_{495} 0.054 after 120 sec (near complete dilution). Note that the Petri dish (35 X 10mm) was used to determine the rate but the lid is used for actual experimental runs.

Perfusion Solution - Artificial Pond Water. The experiments on the pH dependence of the electrical potential of *Eremosphaera viridis* cells used APW (Artificial Pond Water) at different pH's. The abbreviation APW followed by a number indicates APW at the pH indicated by the number. For instance, APW6 indicates APW solution at pH 6. The concentrations of ions in APW are similar to those found in naturally occurring freshwaters (Table III). Stock ion solutions and stock buffer solutions are prepared at 100mM, then diluted to final concentration. APW5 through APW9 were used for perfusion experiments and prepared with buffers appropriate for each pH; the pH was adjusted with 1N NaOH. APW solutions were usually prepared at final volumes of 100mL; approximately 50mL is required for each change in perfusion solution during the pH perfusion protocol.

TABLE III: APW Ion and Buffer Concentrations

	KCl	$CaCl_2$	$MgCl_2$	NaCl	Buffer
Final APW Concentrations (mM)	0.5	0.1	0.1	0.5	1

Holding Pipette Fabrication. The holding micropipettes were prepared by pulling capillaries using a double pull technique to create a blunter tip than that used for cell impalement. The tips were cut by hand, then ground using a micro-grinder (model EG-44, Narashige) to achieve a final diameter of about 120 microns (Figure 4A).

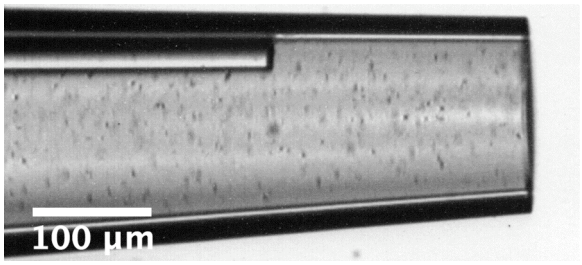

Figure 4A. Cell holding micropipette. The internal filament of the tubing can be seen inside the micropipette. The aperture is adjusted by micro-grinding to about 120 micron, suitable for seating the cells under slight negative pressure.

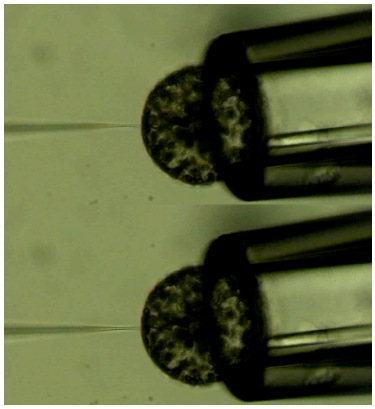

Figure 4B. Cell impalement. In the upper panel, the double-barrel micropipette tip is pressed against the wall and slightly bent. Tapping causes the tip to penetrate the cell (lower panel).

Impalement Protocol. First, a healthy cell (based on spherical shape and green color) was selected and held tightly with the holding pipette. The double-barrel microelectrode was moved under the objective and aligned with the holding pipette. The cell was impaled by slowly moving the tip forward, the tip would often bend when pushed against the wall. Gently tapping once the tip was bent against the cell wall effected impalement of the cell (Figure 4B), confirmed by the change in potential monitored on the oscilloscope.

Determining Current Injection Effects. To rule out any bias in the experiments from the polarity and magnitude of the injected current, it was important to determine 1) if there was long-term damage to cells during injection; 2) different responses to positive or negative current; and 3) different responses to current magnitude (±1nA or ±2nA). The current injection durations were set at 3min. A time lapse of the run was recorded with the Lumenera color camera using the Infinity Analyse program by capturing an image every 10s for 300s. A trace of the current (in nA) and potential (in V) was recorded simultaneously with nidatalogger to determine time of impalement and match current injections with the time lapse images.

pH Perfusion Protocol. Cells were impaled as described above. A picture of the cell was taken for measurement of cell diameter (to calculate cell surface area). Data (current [nA] and voltage [mV]) was collected at a rate of 2 or 4 samples per second. Once successfully impaled with a stable voltage, the perfusion pump was started, first with APW7. For approximately 3min, currents (±1.0nA or ±2.0nA) were injected at intervals

of 20–30s. Then the perfusion solution was changed to APW6 or APW8. After waiting 2min (to allow complete mixing), currents were again injected at 20–30s intervals for 3min. The perfusion solution was changed to APW5 (from APW6) or APW9 (from APW8) and the protocol continued. Finally, the perfusion solution to returned to APW7 for final control measurements. Perfusion was stopped, the cell re-focussed, a picture taken, the double barrel micropipette removed from the cell to obtain an'out-of-cell' potential measurement and data acquisition ended.

For runs 1 to 10, APW solutions were changed by perfusion in the following order: APW7 to APW6 to APW5 to APW7. For runs 11 to 15, APW solutions were changed by perfusion in following order: APW7 to APW8 to APW9 to APW7. For runs 1 to 4, a current of +2.0nA then -2.0nA was injected. For runs 5 to 15, a current of +1.0nA then -1.0nA was injected. For runs 1 to 5, current was injected approximately every 20s for 3min and then potential measured off the digitized trace. For runs 6 to 15, current was injected approximately every 30s for 3.5min and potential peaks were read off oscilloscope. However, data was read off the digitized trace if peaks were off the screen of the oscilloscope. The times at which current was injected is measured off the digitized traces.

RESULTS

pH Dependence of Cell Growth. Cell concentration or cell density of each flask is averaged over three samples taken (Table IV). The mean density of cells is averaged over the three flasks.

Table IV: Example of Cell Count and Density Calculation from Growth Experiment 1

Time (Hrs)	pH	Flask	Sample 1 (# of cells)	Sample 2 (# of cells)	Sample 3 (# of cells)	Average over Samples	Sample Size (mL)	Density (Cells/mL)	Mean Density
46.00	5	1	36	38	74	49.33	0.05	987	902
		2	53	55	49	52.33	0.05	1047	
		3	55	8	38	33.67	0.05	673	
72.00	5	1	78	180	72	110.00	0.05	2200	2142
		2	180	96	145	140.33	0.05	2807	
		3	51	103	59	71.00	0.05	1420	
96.00	5	1	93	172	87	117.33	0.02	5867	3833
		2	104	24	64	64.00	0.02	3200	
		3	37	68	41	48.67	0.02	2433	

By taking the mean density of each pH and plotting over time a clear relation is observed of how well cells grew under different pH (Figure 5). The mean density data for each pH were fitted to a logistic growth curve given by the following:

$$N = \frac{K \bullet N_0 \bullet e^{T/g}}{K + N_0 \bullet e^{T/g} - 1}$$

Where N is the cell density (dependent variable), K is the carrying capacity (maximum number of cells able to grow), N_0 is the initial cell density, T is the time in hours (independent variable), and g is the generation time (time for cell density to double).

Figure 5. Growth curves from mean cell density at different pH. The data points in black or hollow are from the first growth experiment. Data points in gray are taken from the second growth experiment. The mean cell density for each pH experiment is fitted to the logistic growth curve equation.

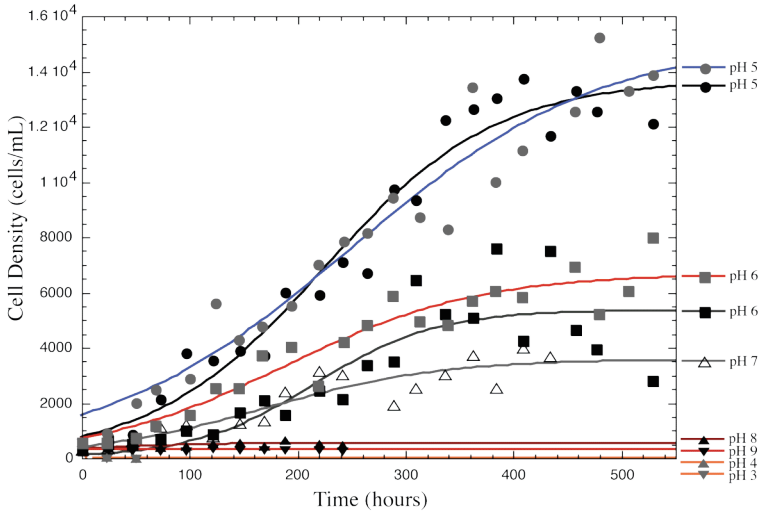

At pH 3 and pH 4, all cells died by day three and day four, respectively. At pH 8 and ph 9 all cells died by day 12 (cells probably died at a much earlier rate because of a

discrepancy in scoring dead and live cells, dead cells might have been recorded as alive). Regardless, the cell density remained constant or declined, showing no growth. Recorded live cells are those with cytoplasm that is green in colour, not retracted from edges, and with no dark coalesced regions.

pH dependence of Carrying Capacity. The carrying capacity (maximal cell density) and generation time can be compared between pH using data from the curve fits (Table V).

Table V: Carrying Capacity (maximal cell density) and Generation Time of Cell Growth at Different pH

pH	Experiment	Carrying Capacity (cells/mL)	Generation Time (hours)
3	1	"0"	No growth.
4	1	"0"	No growth.
5	1	13686 ± 669	80 ± 10
5	2	15179 ± 1346	116 ± 19
6	1	5353 ± 585	56 ± 23
6	2	6673 ± 435	90 ± 17
7	1	3577 ± 445	82 ± 27
8	1	546 ± 54	No growth.
9	1	299 ± 29	No growth.

The generation time or doubling time, which signifies how much pH affects cell division, does not vary over a large range between pH 5, pH 6, and pH 7 (3.3–4.8 days) when considering the range of error. However, pH does show a large effect on the carrying capacity (Figure 6).

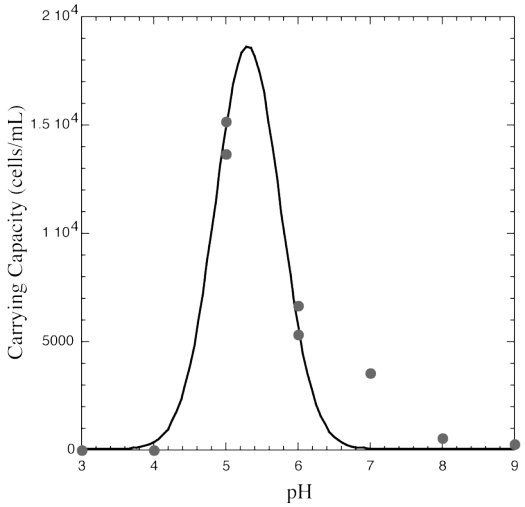

Figure 6. pH dependence of carrying capacity – Guassian fit. Carrying capacity (maximal cell density) is assumed to be zero at pH 3 and pH 4 because of how quickly the cells died. The data points of carrying capacity for the rest of the pH are taken from curve fits over the mean cell density (Figure 3). The carrying capacity is fit to a Gaussian curve. Note the presence of a shoulder at pH 7.

The carrying capacity (K) *versus* pH was fit to a Gaussian or normal distribution with three parameters (the mean, μ, population variance, σ, and maximal carrying capacity, N_{max}):

$$K = N_{\max} \bullet \frac{e^{-(pH-\mu)^2/2\sigma^2}}{\sigma\sqrt{2\pi}}$$

From the fit, the maximum carrying capacity is 16375 ± 21083 cells/ml at a mean pH of 5.3 ± 0.2. However, a normal distribution does not explain the presence of a shoulder at alkaline pH (at pH 7.0). A better fit of the carrying capacity over pH conditions would be to use an interpolation fit (Figure 7).

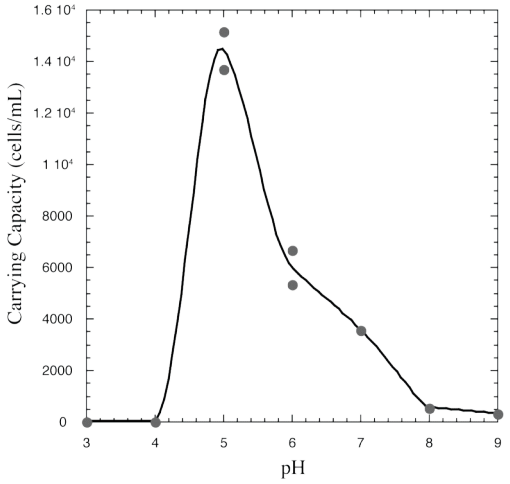

Figure 7. pH dependence of carrying capacity – smoothed curve fit. Carrying capacity is assumed to be zero at pH 3 and pH 4 because of how quickly the cells died. The data points of carrying capacity for the rest of the pH are taken from curve fits over the mean cell density (Figure 3). The carrying capacity is fit to an interpolation where adjacent points are connected by smooth straight lines (in Kaleidagraph).

Comparison of Different Current Injection Conditions. The purpose of this experiment was to determine if there was an advantage between using 1nA or 2nA current, positive and negative current, and electrode solution with or without BAPTA during injection. We did this because we observed cytological rearrangements in preliminary experiments and wanted to determine cause. For each run, current was injected for 3min and a time lapse recorded for 5mins for every 10s including a few frames before and after injection. Using the data trace, a montage is built from the time lapse images with labels for time before, start of, during, end of, and after current (Figure 8).

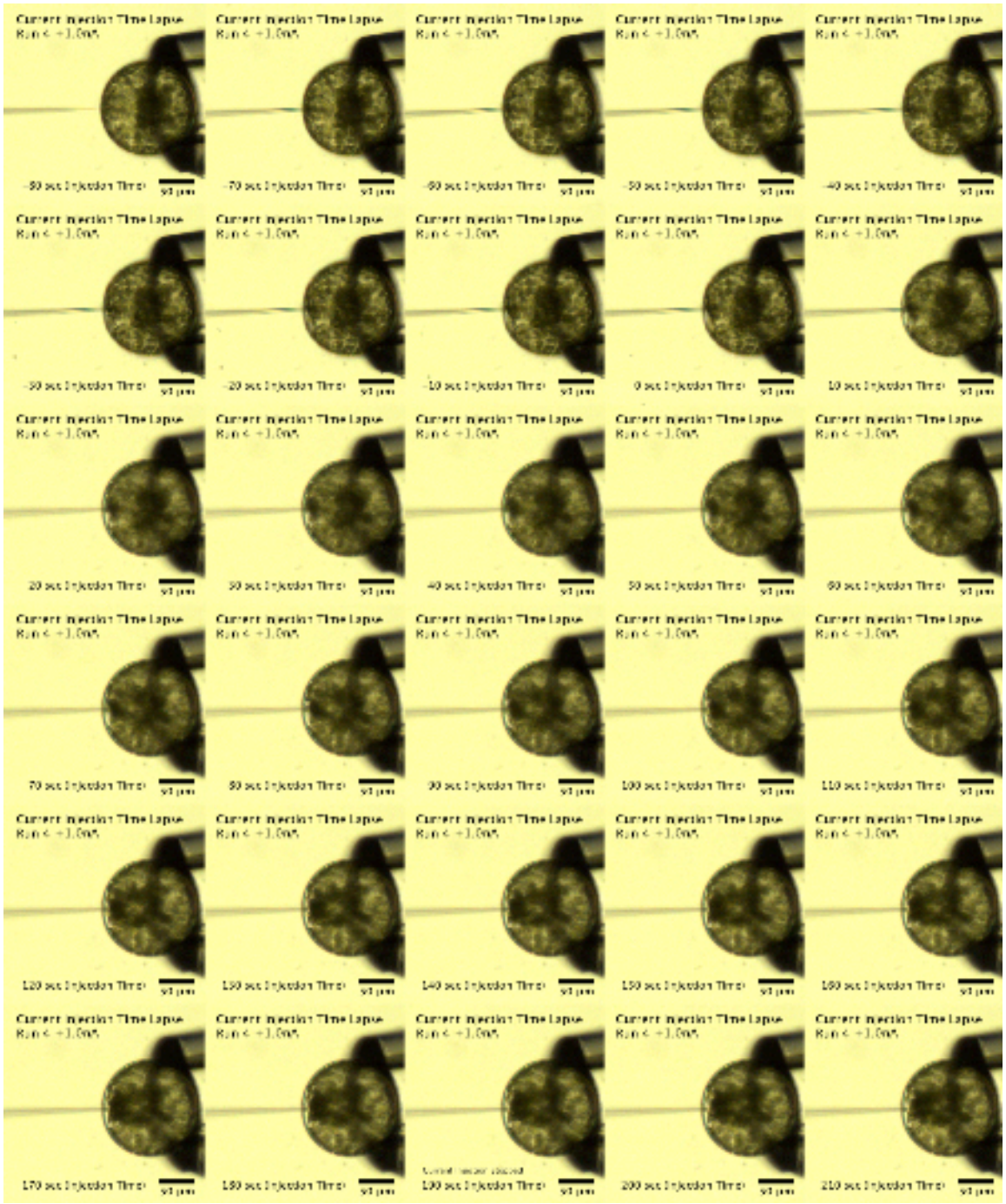

Figure 8. Run 4 of +1.0nA with BAPTA Current Injection. Here is an example of an individual run where the time lapse of every 10s is compiled and information of current injection start and end times are included.

To compare the different run conditions, montages are truncated to show only a few frames, which include frames before current injection and up to the end of current injection (Figure 9).

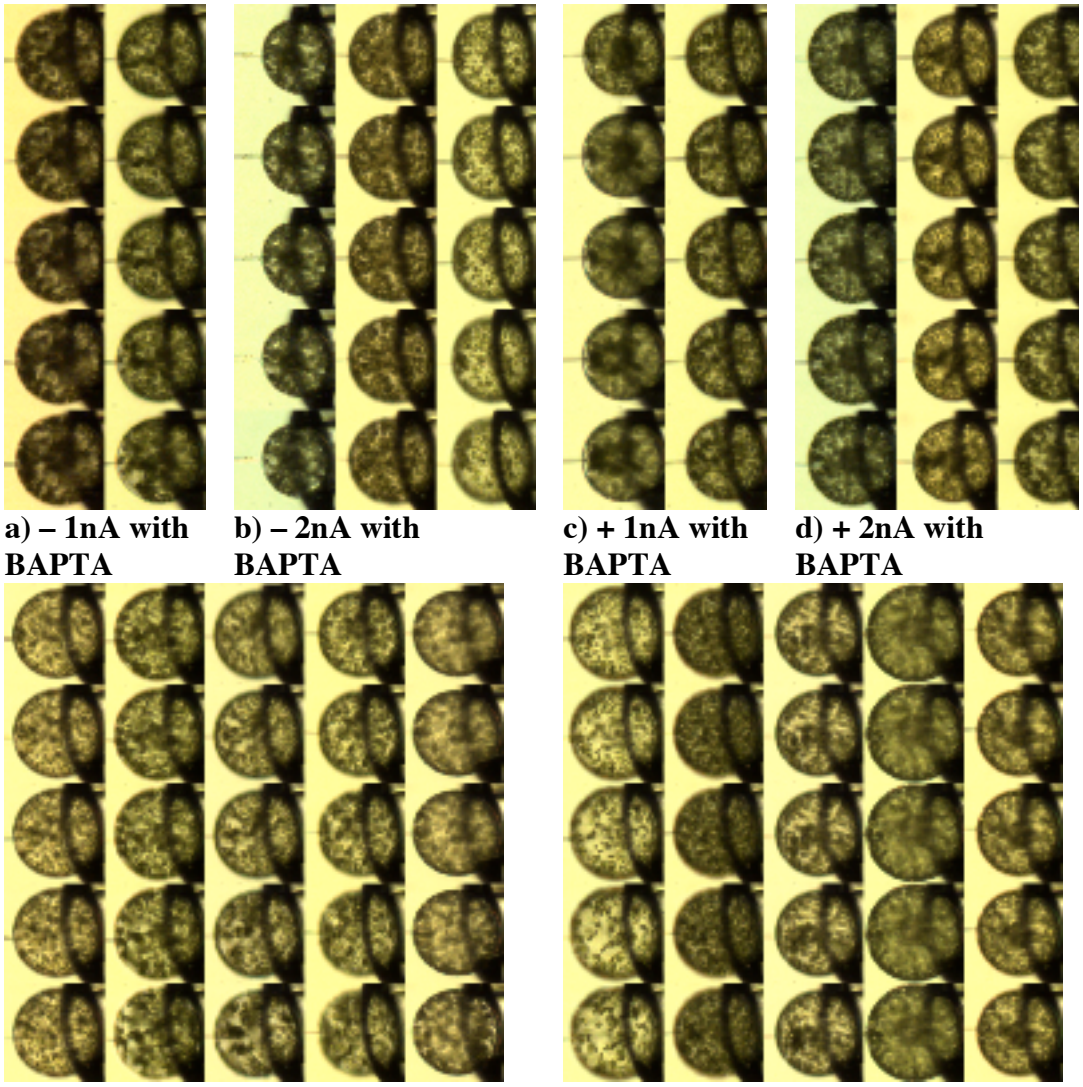

a) – 1nA with BAPTA **b) – 2nA with BAPTA** **c) + 1nA with BAPTA** **d) + 2nA with BAPTA**

e) – 2nA without BAPTA **f) + 2nA without BAPTA**

Figure 9. The frame montages are arranged chronologically vertically down. The top frame is 10s before injection. The second one below is 30s of current injection. The third frame is 60s, the fourth is 120s, and the bottom last frame is 180s of current injection. The amount of current injected is labeled below each set.

a), b), c) and d) were injected with 3M KCl and 1mM K_4BAPTA.

e) and f) were injected only with 3M KCl.

There is no noticeable advantage between 1nA and 2nA, using BAPTA, or between positive and negative current. All conditions had some runs where there was little change and some runs where there was darkening or lightening change in the cells due to cytological re-arrangement.

pH Perfusion. The perfusion experiments involved measuring the potential in the cell and the deflection of the potential during current injection while cells were in APW solutions of different pH. The APW solutions were changed by perfusion to either more acidic APW going from pH 7 to pH 6 to pH 5 and returning to pH 7, or to more basic APW changing from pH 7 to pH 8 to pH 9 and returning to pH 7. The potential and potential deflections were either measured off the trace or read off the oscilloscope and recorded, and matched to the time of injection recorded on the trace. The resistance was calculated from the basic simple circuit relation of:

$$R = \frac{V}{I}$$

Where R is the resistance in MΩ, V is the voltage deflection from the membrane potential in mV, and I is the current in nA. Since resistance decreases as membrane surface area increases, the specific resistance, ρ, is a better unit for comparison and is given by:

$$\rho = R \bullet A$$

where ρ is the specific membrane resistance (in kΩ•cm^2), R is the resistance, and A is the surface area of the cell. The surface area of the cell is approximated by measuring the diameter, D, of the impaled cell and using the relation:

$$A = 4\pi(\frac{D}{2})^2$$

For each current injection, positive and negative current were injected. The resistance is calculated from the voltage deflection from the positive and negative current and the average of these two resistances is used to calculate the specific resistance for each point of current injection. An example of an experiment is shown in Figure 10.

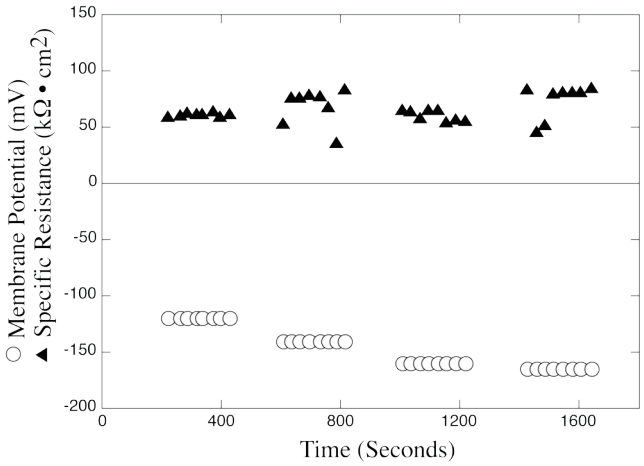

Figure 10. Membrane potential and specific resistance of a perfusion run. This is an example of an individual perfusion run. Each group of data points represent a number of measurements taken to calculate membrane potential and specific resistance at a particular pH. This is data from run 6 where APW pH was changed from 7 to 6 to 5 and back to 7. The break in between groups of data points is the time taken to change APW solution by perfusion.

pH Dependence of Membrane Potential and Specific Resistance. The average of the membrane potential and specific resistance is taken across each group of measurements over a particular pH for each individual run (Figure 11 & 12).

Figure 11. Scatter plot of mean membrane potential for each run. The graphs show the scatter of the mean membrane potential (mV) for each pH during each run.

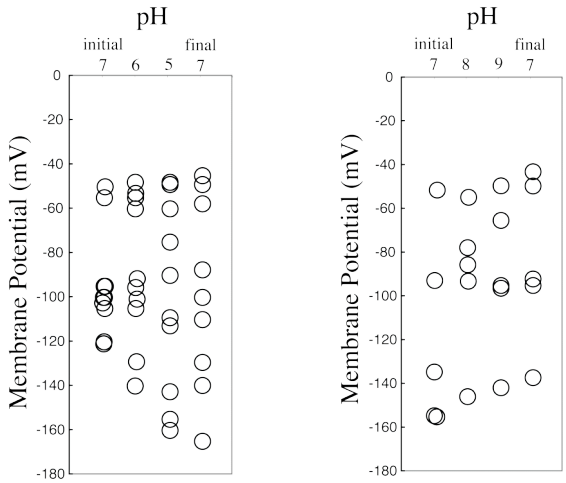

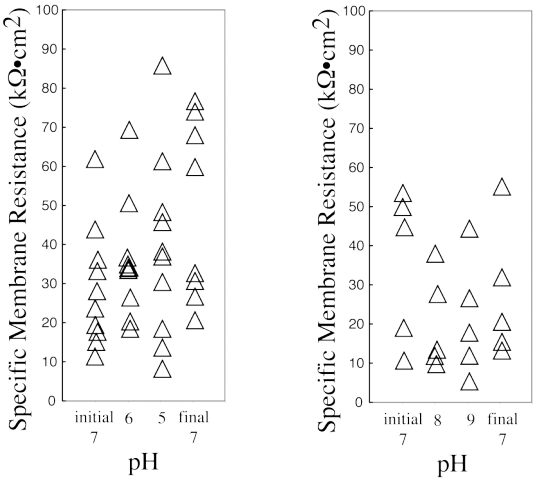

Figure 12. Scatter plot of mean specific resistance for each run. The graphs show the scatter of the mean specific resistance ($k\Omega \bullet cm^2$) for each pH during each run.

To find if there is a correlation between membrane potential and membrane resistance with pH, the mean over all runs and standard error are graphed (see Figure 13 & 14), the t-test is calculated for each pH with initial pH 7 as control (see Table VI & VII), and finally the mean membrane potential at each pH is graphed over the GHK derived relationship (Figure 15)

Figure 13. Mean Membrane Potential. The means were calculated over all runs for each type of perfusion (acidic APW or basic APW) for each pH.

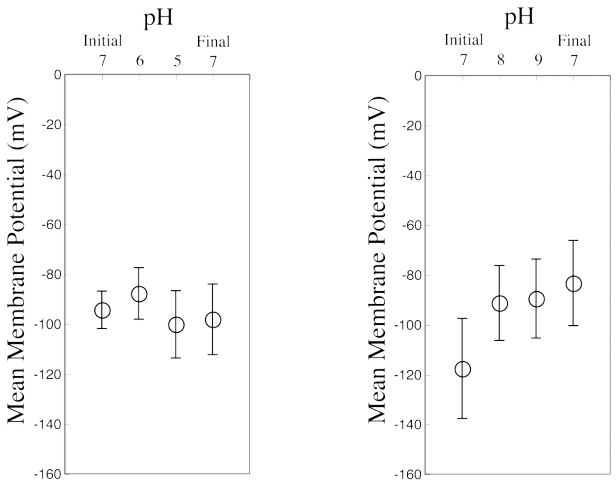

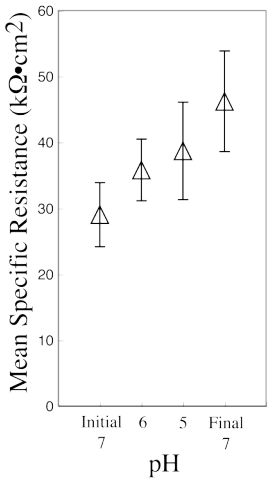

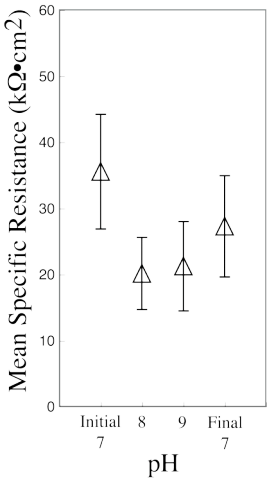

Figure 14. Mean Specific Resistance. The means were calculated over all runs for each type of perfusion (acidic APW or basic APW) for each pH.

In general, both the potential and specific resistance were independent of pH. That is, no t-test comparison revealed a statistically different potential or resistance.

Table VI: T-Test Comparisons of Mean Potential and Mean Specific Resistance of Acidic APW Experiments

pH	Mean Potential	Standard Deviation of Mean Potential	Standard Error of Mean Potential	T-Test of Mean Potential to Initial pH 7	Mean Specific Resistance	Standard Deviation of Mean Specific Resistance	Standard Error of Mean Specific Resistance	T-Test of Mean Specific Resistance to Initial pH 7
7	-94	24	8	N/A	29	15	5	N/A
6	-88	33	10	0.61	36	15	5	0.33
5	-100	43	13	0.71	39	23	7	0.29
7	-98	42	14	0.82	46	23	8	0.078

Table VII: T-Test Comparisons of Mean Potential and Mean Specific Resistance of Basic APW Experiments

pH	Mean Potential	Standard Deviation of Mean Potential	Standard Error of Mean Potential	T-Test of Mean Potential to Initial pH 7	Mean Specific Resistance	Standard Deviation of Mean Specific Resistance	Standard Error of Mean Specific Resistance	T-Test of Mean Specific Resistance to Initial pH 7
7	-118	45	20	N/A	36	19	9	
8	-91	34	15	0.33	20	12	5	0.18
9	-90	35	16	0.31	21	15	7	0.23
7	-83	38	17	0.23	27	17	8	0.49

Figure 15. Comparison of mean membrane potential to GHK derived membrane potential. The mean membrane potentials are graphed with standard error (see Table VI and Table VII) over the GHK function of membrane potential specific to internal and external conditions of *Eremosphaera viridis* in these experiments. Proton concentration, $[H^+]$ is in log scale and in mol/L. Equivalent pH scale is marked underneath.

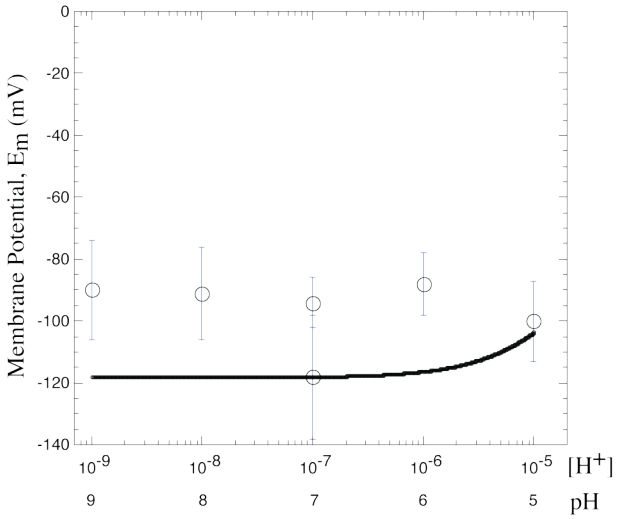

Relationship between Membrane Potential and Specific Resistance. Data from the pH runs were compiled to examine the relation between potential and the specific resistant (Figure 16). There was a linear relationship: A large resistance (that is, a small conductance) corresponded to a hyperpolarized membrane potential for experimental runs at either acidic APW or basic APW.

Figure 16. Membrane Potential vs. Specific Resistance. The mean values of membrane potential graphed against associated specific resistance. The top graph compiles data for runs at acidic pH (APW pH 7–5). The bottom graph compiles runs at basic pH (APW pH 7–9).

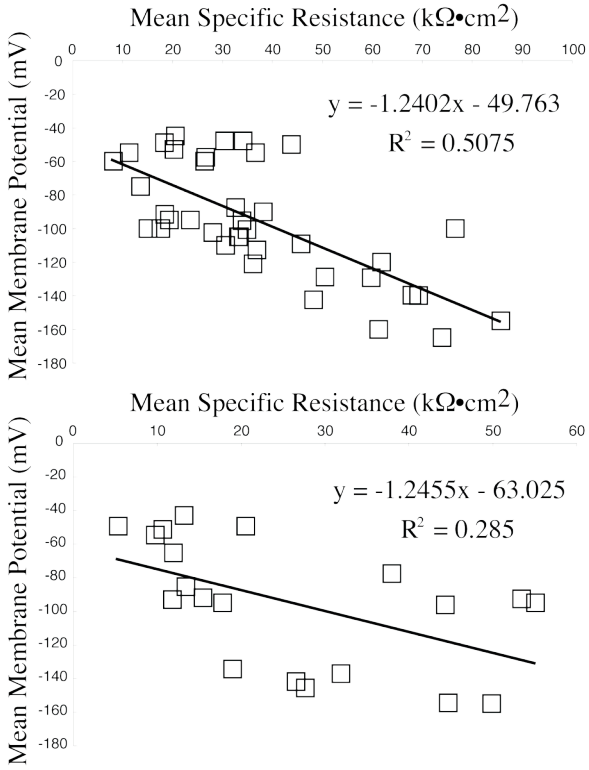

DISCUSSION

The pH growth experiments show that *Eremosphaera viridis* is an acidophile, with maximal growth at pH 5. There was a sharp decline in carrying capacity at pH 4, a more gradual one at pH 6 to pH 7. However the doubling time across pH values of observable growth (5, 6, and 7) did not vary greatly. It was in a range of 3.3 to 4.8 days. These effects are not due to changes in the medium pH, which was fairly constant, changing to slightly alkaline (about 0.2 units) at end of growth experiments.

Current injection experiments allowed us to determine whether there was any damaging effect on the algal cells. There was no consistent effect of the size of the current (2nA or 1nA), positive or negative current (K^+ ions vs. Cl^- ions), or whether BAPTA (a calcium chelator) was present. None of these can be identified as the cause of cytoplasmic re-arrangement that was sometimes observed after impalement.

Changing the pH over the range 5 to 9 had no effect on the membrane potential or specific resistance when either acidic (stepwise change from pH 7 to pH 6 to pH 5 back to pH 7) or basic (stepwise change from pH 7 to pH 8 to pH 9 back to pH 7) pH perfusion was performed. Membrane potential varies over a range of -40mV to -170mV and the specific resistance ranged from 10kΩ·cm^2 to 90 kΩ·cm^2 respectively. Plotting the mean potentials graphed with GHK membrane potential function showed that the potentials are not expected to vary that much from a theoretical standpoint, nor do they experimentally. The t-tests of perfusion APW to initial APW of pH 7 (Table VI and Table VII) supports the idea of no observable differences of membrane potential and specific resistance caused by changing the pH of APW solution as all the t-tests yielded probabilities of greater than 5% of differences.

There is a linear relationship between specific resistance and membrane potential where at low specific resistance there is low membrane potential, and at high specific resistance there is high membrane potential. This suggests that two different electrical states exist. In one, with low specific resistance (that is, with higher conductance), the potential is depolarized; at high specific resistance (that is, low conductance), the potential is hyperpolarized. This may be due to a varying contribution of a cation conductance to the cell potential. To determine this experimentally, experiments modifying the concentrations of cation (K^+ and Na^+) would have to be performed.

In summary, the alga *Eremosphaera viridis* is confirmed to be an acidophile. Its electrical properties are relatively insensitive to pH either acidic or alkaline.

REFERENCES

Bethmann, B. and Schönknecht, G. (2009) pH regulation in an acidophilic green alga – a quantitative analysis. *New Phytol*. 183: 327–339.

Bethmann, B., Thaler, M., Simonis, W. and Schönknecht, G. (1995) Electrochemical potential gradients of H^+, K^+, Ca^{2+} and Cl^- across the tonoplast of the green alga *Eremosphaera viridis*. *Plant Physiol*. 109: 1317–1326.

Bethmann, B., Simonis, W. and Schönknecht, G. (1998) Light-induced changes of cytosolic pH in *Eremosphaera viridis*: recordings and kinetic analysis. *Plant Physiol*. 49: 1129–1137.

Dillon, P.J., Reid, R.A. and de Grosbois E. (1987) The rate of acidification of aquatic ecosystems in Ontario, Canada. *Nature* 329: 45–48.

Frey, N., Buchner, K-H. and Zimmerman, U. (1988) Water transport properties and regulatory processes in *Eremosphaera viridis*. *J. Memb. Biol*. 101: 151–163.

Köhler, K., Geisweid, H-J., Simonis, W. and Urbach, W. (1983) Changes in membrane potential and resistance caused by transient increase of potassium conductance in the unicellular green alga *Eremosphaera viridis*. *Planta* 159: 165–171.

Köhler, K., Steigner, W., Simonis, W. and Urbach, W. (1985) Potassium channels in *Eremosphaera viridis*. I. Influence of cations and pH on resting membrane potential and on an action-potential-like response. *Planta* 166: 490–499.

Köhler, K., Steigner, W., Kolbowski, J., Hansen, U-P., Simonis, W. and Urbach, W. (1986) Potassium channels in *Eremosphaera viridis*. II. Current- and voltage-clamp experiments. *Planta* 167: 66–75.

Lew, R. R (2006) Double barrel micropipettes for voltage clamp of intact turgid plant and fungal cells. In Volkov AG (ed.) Plant Electrophysiology – Theory and Methods. Springer Verlag. Berlin Heidelberg. pp 139–154.

Linz, K.W. and Köhler, K. (1994) Vacuolar ion currents in the primitive green alga *Eremosphaera viridis*: the electrical properties are suggestive of both the Characeae and higher plants. *Protoplasma* 179: 34–45.